Neutron response functions and detection efficiency of a spherical proton recoil proportional counter

WANG Xinhua* HE Tie GUO Haiping AN Li ZHEN Pu
MOU Yunfeng YANG Jian

Institute of Nuclear Physics and Chemistry, Chinese Academy of Engineering Physics, Mianyang 621900, China

Abstract The neutron response function and detection efficiency of a spherical proton recoil proportional counter (SP) play key roles in precise measurement of neutron spectra of the interior materials. In this paper, the response functions and detection efficiency of three SPs developed at CAEP are simulated by Geant4. The simulated spectra are compared with pulse-height spectra measured at 0.165, 0.575, 1.4, and 14.1 MeV of incident neutrons. And the calculated detector efficiencies agree within 5% with the data obtained by neutron activation.

Key words Spherical proton recoil proportional counter, Response function, Detection efficiency, Geant4.

1 Introduction

Spherical proton recoil proportional counters (SPs) operating in an energy range from a few tenth of a keV to a few MeV have been used as neutron spectrometer in weapon laboratories and metrological institutes since 1960s[1–3]. Being independent of the anisotropy distribution of incident neutron fluence, and of high-energy resolution, the SPs can collect neutron spectra of materials inside a medium. The SPs response functions, as key roles in measuring the neutron spectrum, are determined by simulation owing to the scarcity of mono-energy neutron sources.

In pioneering software packages, such as SPEC, SPHERE and MCNPX, designed for SPs[1,4–7], the wall effect was taken into consideration, but the electric field effect was not considered completely. The Geant4 code, a open-source and general-purpose Monte Carlo simulation toolkit[8–11], may be applied to explore a response function of SP inside a non-uniform electric field. In this study, the neutron response functions and detection efficiency of SPs were measured and calculated by Geant4 in an incident neutron energy range of 0.01–16 MeV. The spectra simulated at 0.165, 0.576, 1.4, and 14.1 MeV were compared with experiment data, so as to determine the absolute detection efficiencies, and the neutron flux at the detector position was further measured by neutron activation method.

2 Methods

2.1 The three SPs developed at CAEP

A schematic drawing of the SPs developed at CAEP according to Benjamin type[1] is shown in Fig.1. The outer and inner diameters of the spherical counter were 30 and 28 mm, respectively. The anode was gold-plated tungsten of 0.0125-mm length, and its inner wall incorporated with a uranium source was used for energy calibration. Two SPs were filled with a mixture of 95% H_2 and 5% CH_4 at 0.3 and 0.5 MPa, for detecting 0.1–0.4- and 0.2–0.8-MeV incident neutrons, respectively. Another SP was filled with CH_4 at 0.5 MPa to detect 0.6−2.0 MeV neutrons.

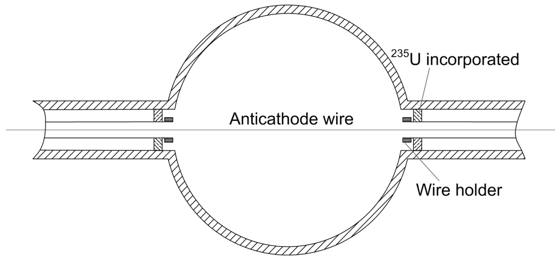

Fig.1 **A** schematic diagram of the spherical proton recoil proportional counter.

* Corresponding author. *E-mail address:* sword1224@163.com
Received date: 2010-05-15

2.2 MC simulation with Geant4

The neutron response function and detection efficiency of the SPs were calculated with the Geant4 toolkit, taking account geometry of the entire container, the electric field in the inner detector, the chemical composition, and the gas pressure. The Geant4 simulation of neutron transport was from thermal energies to 20 MeV. Neutron capture, fission, elastic and inelastic scatting were examined by referring to the ENDF-B-VI cross-section data. The transported ions included proton, alpha particle, and generic ions. Assuming that the same energy loss of charged hadrons can induce the same number of electron-ions, the pulse-height spectrum was obtained by the energy deposition of the ions of p, α, ^{12}C, ^{9}Be etc., which were formed by the neutron interactions with the gas and the stainless steel wall. The neutron response function and detection efficiency were calculated with the following assumption: (1) the neutron source was 30 cm away from the SP center, and neutrons was emitted in a cone-shaped distribution; (2) the calculation model was simplified, and the anode connector was neglected; (3) the neutron energies were homophonic; and (4) The edge and the non-uniform electric field effect were considered.

The energy range up to 2 MeV was calculated in 10 keV steps, which is precisely enough to measure the energy distribution by the counters. The calculation could be in 0.25 MeV steps in 2–16 MeV, where the recoil protons lose only a fraction of energy in the detector gas and the energy contribution can be eliminated by down-scattering correction. The pulse-height spectrum along its axis was divided into 2000 channels, and each channel had an energy bin width of the 10 keV.

2.3 The measurements

The pulse-height spectra induced by a mono-energy neutron beam were compared with the calculation results. Proton beams at E_p=1.2, 1.4, and 2.2 MeV, were delivered from the 2.5 MeV tandem Van de Graaf at Institute of Nuclear Science and Technology, Sichuan University. TiT and Be targets were bombard to produced low energy neutrons via the $T(p,n)^3He$ and Li(p,n)Be reactions. And a deuterium beam with 200 keV, delivered from an ns-200 neutron generator at Institute of Nuclear Physics and Chemistry, CAEP, was used to bombard a TiT target and produce high energy neutrons via $T(d,n)^4He$ reaction. The TiT target was cooled by water droplets, so as to minimize tritium escape due to the target-heating effect. The detectors were 30 cm away from the neutron source at an angle of 0° relative to the beam axis. In each case, the separation of the neutron-induced events from the gamma-ray events was neglected. Treated by a preamplifier, a main amplifier, and a gated integrator, the SP signals were introduced into an analog-to-digital convertor of a multichannel analyzer. After the background contribution of the scattered neutrons emitted by the target was subtracted by an appropriate shadow shield of cone between the neutron source and the detector, the net spectrum corresponding to the neutron spectral fluence was determined by the ^3He proportional counter and neutron activation.

3 Results and discussion

3.1 The electric field effect

The electric field affected gas amplification and the deposited energy of recoil ions, so Geant4 simulation with or without the electric field was performed with the 0.5-MPa CH_4 SP and 1.2 MeV incident neutrons. As shown in Fig.2, without the electric field, the gas amplification was lower than with the electric field, and the events of low energy deposition are more than the high energy deposition. But all the events cause a response slope to increase. The result shows that the precise response function of the counter is affected by the non-uniform electric field.

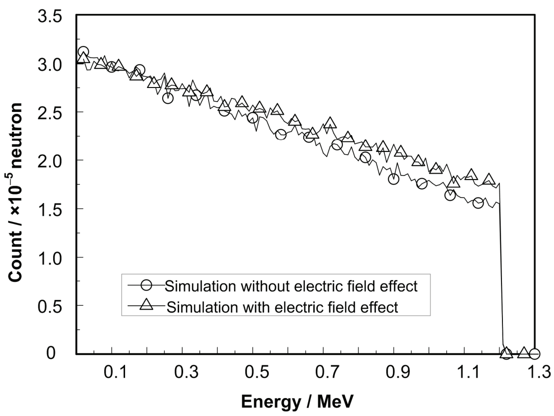

Fig.2 Simulated response function in 0.5 MPa CH_4 SP at 1.2 MeV of incident neutrons with and without the electric field.

3.2 Neutron-response function

In Figs.3 (a)−(c) the simulated response functions at 0.165, 0.576 and 1.4 MeV of incident neutrons, with the energy resolution treated by a Gaussian fitting, agree well with the normalized experimental data, except the low-energy part of the pulse-height spectra, which may be caused by electronic noise and energy deposition of *γ*-rays on the inner surface of the counters. For the 14.1 MeV incident neutrons in Fig.3(d), the contribution to response functions exceed the measurement range of SP system, because of the heavy-charged ions (alpha particles) and fission fragments generated from the spontaneous fission of ^{235}U, and the reaction of the neutrons with carbon nucleus.

3.3 Neutron-detection efficiency

From Fig.3, it can be sure that the SPs are suitable for measuring the pulse-height spectra of incident neutrons in 0.05−2 MeV, and the detection efficiencies at different pressures and incident neutron energies can be in good agreement with the calculated response functions by Geant4, but the energy bin for incident neutrons of high energy neutrons should be larger in the calculation. Fig. 4 shows that all the neutron-detection efficiencies decrease sharply with increasing incident energies up to 3 MeV, where they begin to become almost steady. Comparatively, the more CH_4 at high pressure, the larger detection efficiencies are. And the influence of CH_4 composition on the detection efficiency increases with energy of incident neutrons. The calculated detector efficiencies agreed within 5% with the data obtained by neutron activation (not shown).

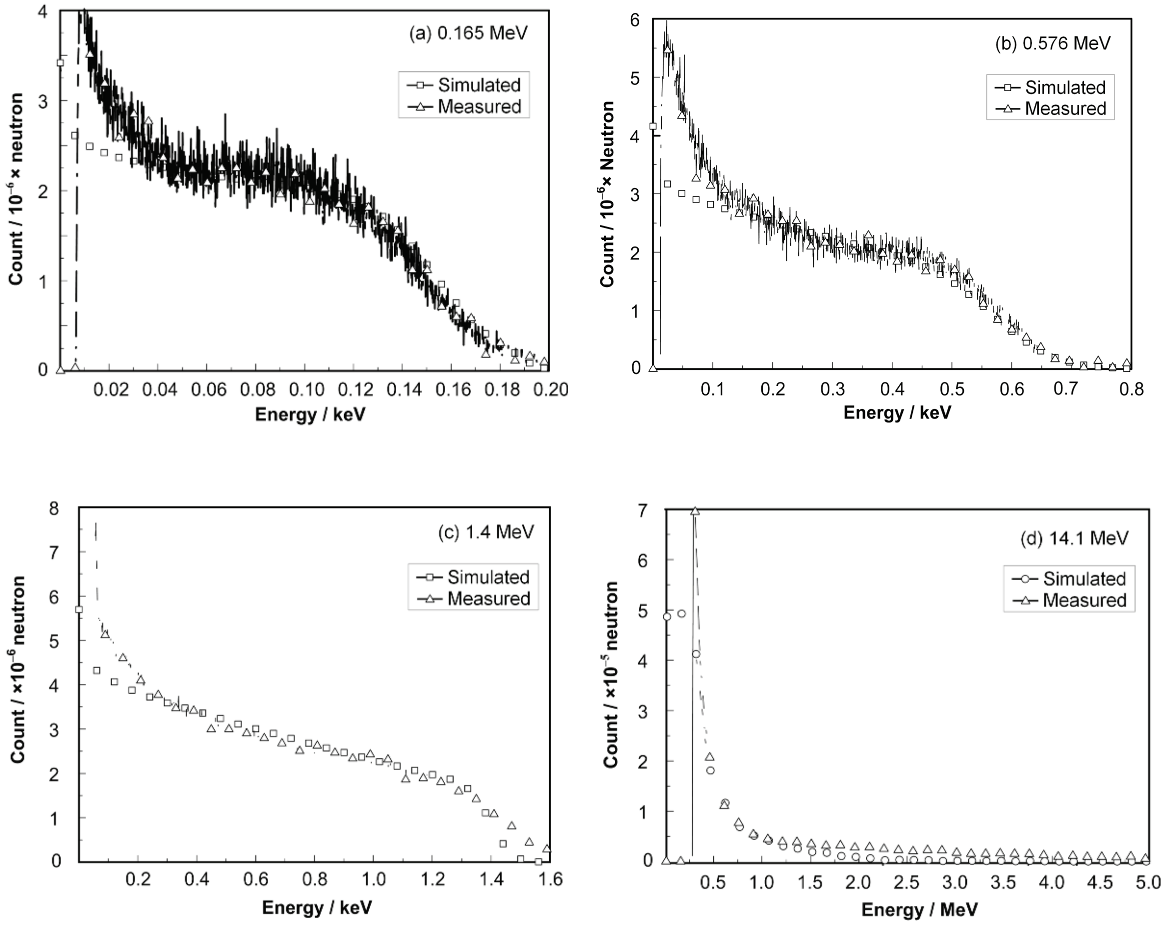

Fig.3 Simulated response functions and the measured pulse-height spectra with incident neutrons of different energies.

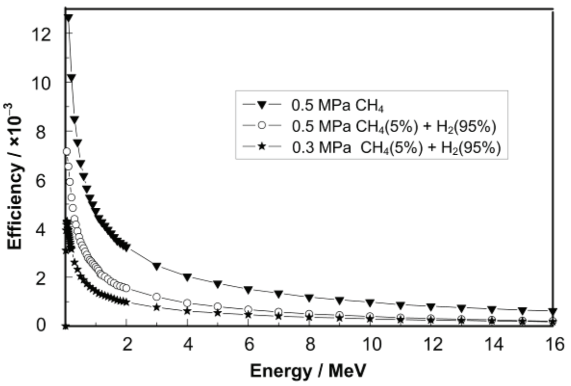

Fig.4 Neutron-detection efficiency of the spherical hydrogen proportional counters.

4 Conclusions

The response function and the detection efficiency of the SPs were simulated by Geant4 for neutrons of 0.01–16 MeV. Experiments at 0.165, 0.576, 1.4 and 14.1 MeV of incident neutrons were performed to check the calculation. The experimental response functions at the low energies agreed well with the simulation results. All the response functions can be determined from the neutron pulse-height spectra. For the 14.1 MeV incident neutrons, however, the simulated response functions differed greatly from the measured pulse-height spectra, owing to the contribution of alpha particles and fission fragments.

Acknowledgements

The authors gratefully acknowledge the assistance of the staff of tandem Van de Graaf facility at Institute of Nuclear Science and Technology, Sichuan University, and the ns-200 neutron generator at Institute of Nuclear Physics and Chemistry, CAEP during the experiments. And we wish to express gratitude to Prof. Yuan Chen and Prof. Xiaobing Luo for their help in the work.

References

1 Benjamin P W, Kemshall C D, Redfearn J. AWRE Report NR2/64, 1964.
2 Benjamin P W, Kemshall C D, Redfearn J. Nucl Instrum Meth, 1968, **59:** 77–85.
3 Birch R, Delafield H J, Parks C A. Radiat Protect Dosimet, 1988, **23:** 281–284.
4 Knauf K, Vorbrugg W. Nucl Instrum Meth, 1991, **A305:** 419–426.
5 Knauf, K, Heimann, C, Kaldune, N, *et al.* PTB-6.42-97-2, 1997.
6 Knauf K, Weurauch M, Simon F, *et al.* PTB-6.42-98-1, 1998.
7 Waters L S, Ed. MCNPX-Uers's manual, version 2.5.0, Los Alamos National Laboratory report. LA-CP-05-0369, 2005.
8 Weise K, Weyranch M, Knauf K. NIM, 1991, **A309:** 287–29.
9 Agostinelli S, Allison J, Amako K, *et al.* NIM, 2003, **A506:** 250–303.
10 Benmosbah M, Groetz J E, Crovisier P, *et al*. Proceedings of Science International workshop on Fast Neutron Detectors and Applications, FNDA, 2006.
11 Patronis N, Kokkoris M, Soudi D G, *et al.* NIM, 2007, **A578:** 351–335.